iScience

CellPress
OPEN ACCESS

Article

Sulfonamide functional head on short-chain perfluorinated substance drives developmental toxicity

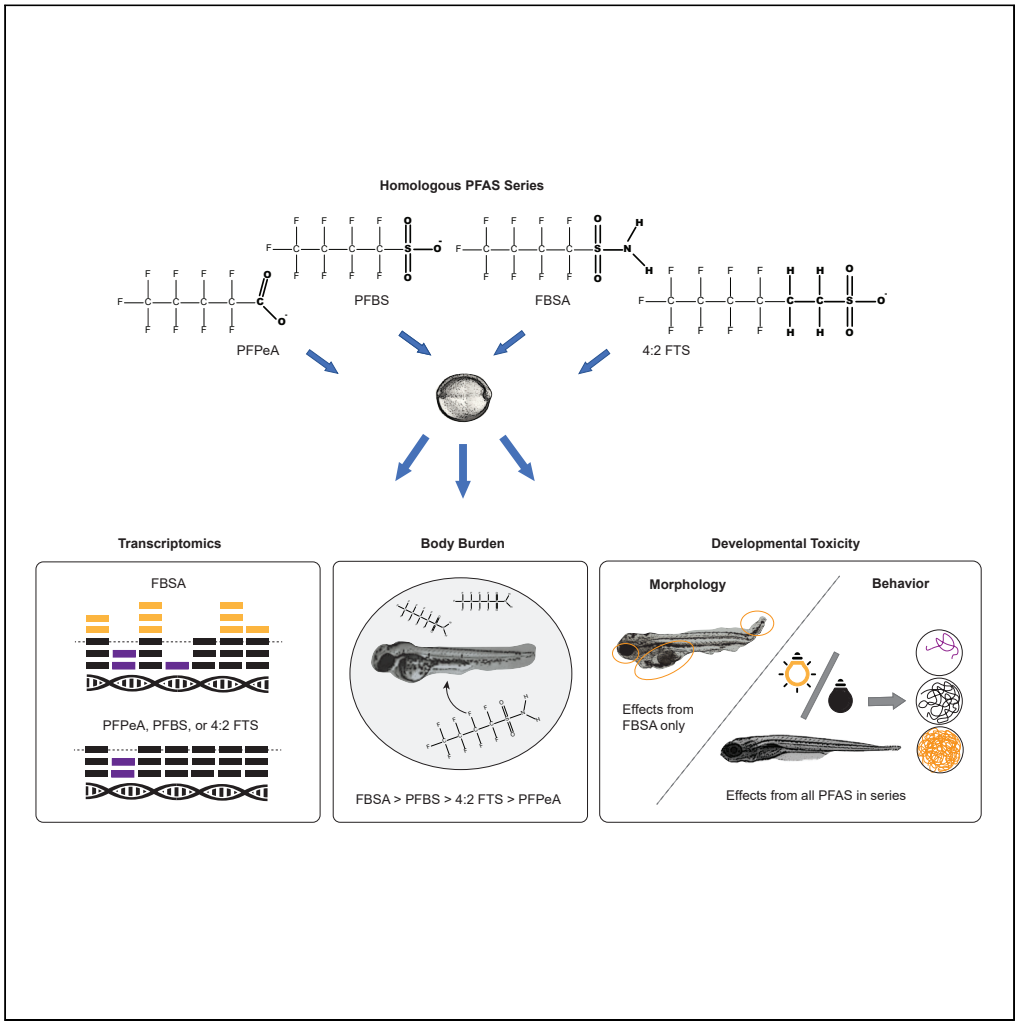

Yvonne Rericha, Dunping Cao, Lisa Truong, Michael T. Simonich, Jennifer A. Field, Robyn L. Tanguay

robyn.tanguay@oregonstate.edu

Highlights

Perfluorobutane sulfonamide (FBSA) was the most developmentally toxic and bioaccumulative in a homologous series

FBSA, PFBS, PFPeA, and 4:2 FTS induced abnormal larval behavior

FBSA exposure induced transcriptional changes that preceded morphological effects

Rericha et al., iScience 25, 103789
February 18, 2022 © 2022 The Authors.
https://doi.org/10.1016/j.isci.2022.103789

iScience

CellPress
OPEN ACCESS

Article

Sulfonamide functional head on short-chain perfluorinated substance drives developmental toxicity

Yvonne Rericha,[1,2] Dunping Cao,[3] Lisa Truong,[1,2] Michael T. Simonich,[1,2] Jennifer A. Field,[1] and Robyn L. Tanguay[1,2,4,*]

SUMMARY

Per- and polyfluoroalkyl substances (PFAS) are ubiquitously detected in environmental and biological samples and cause adverse health effects. Studies have predominately focused on long-chain PFAS, with far fewer addressing short-chain alternatives. This study leveraged embryonic zebrafish to investigate developmental toxicity of a short-chain series: perfluorobutane sulfonate (PFBS), perfluoropentanoic acid (PFPeA), perfluorobutane sulfonamide (FBSA), and 4:2 fluorotelomer sulfonic acid (4:2 FTS). Following static exposures at 8 h postfertilization (hpf) to each chemical (1–100 μM), morphological and behavioral endpoints were assessed at 24 and 120 hpf. Only FBSA induced abnormal morphology, while exposure to all chemicals caused aberrant larval behavior. RNA sequencing at 48 hpf following 47 μM exposures revealed only FBSA significantly disrupted normal gene expression. Measured tissue concentrations were FBSA > PFBS > 4:2 FTS > PFPeA. This study demonstrates functional head groups impact bioactivity and bioconcentration.

INTRODUCTION

Per- and polyfluoroalkyl substances (PFAS), a class of anthropogenic contaminants, are widely recognized as a human health concern owing to ubiquitous detection in environmental and biological media and the adverse health effects they cause. Their unique carbon-fluorine bonds impart highly desirable properties for use in industrial and consumer products (e.g., chemical stability, low reactivity, and the ability to lower aqueous surface tension), which have led to PFAS use across industries, such as aerospace, electronics, energy, textiles, food packaging, medical, and pharmaceuticals (Gluge et al., 2020). This unique chemistry also means that parent compounds and their terminal degradation products are highly persistent in the environment, hence their ubiquitous detection around the globe (Blum et al., 2015). Humans are widely exposed to PFAS through drinking water, diet, and air, and studies around the world have detected these compounds in blood samples. Some PFAS are bioaccumulative, and exposures to some cause a broad range of health effects related to immune and thyroid function, liver and kidney disease, and developmental and reproductive outcomes (Fenton et al., 2021).

Most of our knowledge about PFAS occurrence and toxicity is derived from studies of long-chain compounds (Ateia et al., 2019), with a spotlight on short-chain PFAS only recently emerging. Slight variations in the definition of "short-chain" exist depending on the publication or regulatory agency; however, it is widely accepted that PFAS containing four to six fully fluorinated carbons are considered short-chain (Wang et al., 2017; Ateia et al., 2019; Li et al., 2019). With voluntary phase-out and regulation of legacy long-chain chemicals, specifically perfluorooctanesulfonic acid (PFOS) and perfluorooctanoic acid (PFOA), manufacturers have adopted shorter-chain alternatives (Blum et al., 2015; Brendel et al., 2018). Production and environmental release of short-chain PFAS have been increasing, and this trend is expected to continue (Ateia et al., 2019; Li et al., 2019). In addition to purposeful production and use in consumer products, the extent of which is difficult to know, short-chain PFAS may form via numerous degradation pathways of longer-chain precursors; thus, several studies have detected short-chain PFAS at higher concentrations than long-chain counterparts in various environmental media (Ateia et al., 2019). Perfluorobutane sulfonate (PFBS), perfluoropentanoic acid (PFPeA), perfluorobutane sulfonamide (FBSA), and 4:2 fluorotelomer sulfonic acid (4:2 FTS) are a short-chain homologous series and have been widely detected

[1]Department of Environmental and Molecular Toxicology, College of Agricultural Sciences, Oregon State University, Corvallis, OR 97333, USA

[2]Sinnhuber Aquatic Research Laboratory, College of Agricultural Sciences, Oregon State University, Corvallis, OR 97333, USA

[3]Department of Chemistry, College of Science, Oregon State University, Corvallis, OR 97333, USA

[4]Lead contact

*Correspondence: robyn.tanguay@oregonstate.edu

https://doi.org/10.1016/j.isci.2022.103789

This is an open access article under the CC BY-NC-ND license (http://creativecommons.org/licenses/by-nc-nd/4.0/).

in the environment. PFBS and PFPeA are among the most frequently detected members of this chemical class worldwide, with concentrations ranging from not detected to 4,520 and 254 ng/L, respectively, based on studies spanning the past two decades (Li et al., 2019). FBSA and 4:2 FTS, while not as extensively studied, have also been detected with high frequency in surface and tap waters (Li et al., 2022) and biota (FBSA) (Chu et al., 2016).

Despite manufacturing trends, short-chain alternatives are not necessarily a better option: many short-chain compounds are still highly persistent, resistant to biological and chemical degradation, and their greater solubility in water results in higher mobility in the environment (Brendel et al., 2018; Ateia et al., 2019). Short-chain PFAS also exhibit higher placental transfer efficiency compared to legacy compounds, illustrating the importance of understanding short-chain PFAS toxicity (Gao et al., 2019; Cai et al., 2020). Our knowledge of the full extent of their hazard potential and the mechanisms by which they induce toxicity is still lacking (Ateia et al., 2019; Li et al., 2019).

Embryonic zebrafish (*Danio rerio*) is effective *in vivo* model for the rapid evaluation of chemical toxicity and prioritization of chemical hazard, serving to fill the niche between *in vitro* and mammalian models (Truong et al., 2011; Padilla et al., 2012). They are particularly amenable to toxicological assessments owing to their high fecundity, rapid *ex vivo* development, and embryonic translucence (Horzmann and Freeman, 2018). Zebrafish enable the investigation of complex biological responses while also serving as a platform to probe molecular mechanisms by which contaminants induce toxicity, as their genome is fully sequenced and highly annotated (Howe et al., 2013). Zebrafish are also a translatable model for human health; more than 70% of human protein-coding genes have at least one ortholog in zebrafish, they are amenable to genetic manipulation, and we share highly conserved developmental and biological pathways (Howe et al., 2013). Thus, embryonic zebrafish are a well-suited model to investigate PFAS hazard and toxicity mechanisms.

Several studies have utilized zebrafish to investigate PFAS toxicity, including short-chain compounds with a predominate focus on perfluorinated carboxylic acids and sulfonic acids, but none have systematically interrogated a homologous series also including sulfonamides and fluorotelomer sulfonic acids. Previous studies reported no morphological or behavior effects following PFBS or PFPeA exposure in developmental zebrafish (Menger et al., 2019; Gaballah et al., 2020; Dasgupta et al., 2020). However, varying experimental designs between studies warrant further testing of short-chain homologous series in a single, highly controlled exposure and assessment paradigm. Considering available transcriptomic data in a variety of species, 12 short-chain PFAS elicited gene expression disruptions, including PFBS, perfluorobutanoic acid (PFBA), and PFPeA, as queried using the Comparative Toxicogenomics Database (Davis et al., 2021). The majority of these studies employed techniques such as qPCR or microarrays, and several were *in vitro*. Among the studies to investigate PFBS, only one by Sant et al. used RNA sequencing (RNA-seq) and developmental zebrafish as a model, showing that PFBS exposure elicited the disruption of lipid homeostasis along with a range of phenotypes, including caudal fin malformations and impaired yolk utilization (Sant et al., 2019). RNA-seq is a powerful and unbiased tool increasingly utilized to anchor phenotypes of exposure to changes in the transcriptome (Qian et al., 2014; Yao et al., 2019). An essential step toward elucidating the mechanisms by which less-studied short-chain PFAS induce toxicity is to investigate additional compounds using RNA-seq in a complex *in vivo* system.

In the present study, we leveraged embryonic zebrafish to compare the toxicity of a short-chain homologous series, all containing four fully fluorinated carbons and differing by functional head group: PFBS, PFPeA, FBSA, and 4:2 FTS. We specifically aimed to interrogate the toxicological implications of PFAS functional head groups, assessing morphology and behavior endpoints across a range of nominal concentrations (0-100 μM) and employing our high throughput screening platform previously used to evaluate extensive chemical libraries (Truong et al., 2014, 2020; Geier et al., 2018). The nominal concentration range is higher than levels typically detected in the environment, but these studies are also temporally short and are aimed at systematically comparing chemical toxicity as a function of the functional head group. We then conducted a transcriptomic investigation using mRNA-sequencing (mRNA-seq) to begin to identify mechanisms of toxicity. To understand developmental and transcriptional effects in the context of internal chemical concentration, we also measured chemical body burdens. We demonstrate the utility of a structurally guided assessment of PFAS using developmental endpoints and transcriptomics in zebrafish to identify differences in toxicity.

Table 1. The homologous series impacted larval behavior, only FBSA impacted morphology[a]

PFAS	Adjusted Exposure Concentration (μM)	Significant % Morphological Effect	LPR Dark	LPR Light
FBSA	100	97	NA	NA
	78	92	NA	NA
	37	50	NA	NA
	17	–	HYPO	HYPO
	6.8	–	HYPO	–
	2.7	–	HYPO	HYPO
	1.0	–	HYPO	HYPER
PFBS	57	–	–	HYPER
	43	–	–	HYPO
	20	–	–	–
	9.3	–	–	–
	3.7	–	–	–
	1.4	–	–	–
	0.6	–	–	–
PFPeA	69	–	HYPER	–
	52	–	–	–
	24	–	HYPER	HYPO
	11	–	HYPER	HYPO
	4.4	–	–	HYPO
	1.7	–	–	–
	0.7	–	–	–
4:2 FTS	85	–	–	HYPO
	64	–	–	HYPO
	30	–	–	–
	14	–	HYPO	HYPER
	5.5	–	–	–
	2.2	–	–	HYPER
	0.9	–	–	–

[a]Adjusted exposure concentration was calculated from analytically measured stock concentrations. Any morphological effects percentage represents the totality of all morphological endpoints, and all percent incidence below 20 are indicated by dashes. Larval photomotor response in the dark period of the assay (LPR Dark) and the light period (LPR Light) columns show behavior activity: dashes within a cell indicate lack of significant behavior effects compared to the control group, HYPO indicates hypoactivity, HYPER indicates hyperactivity, and NA means that high morphological effects did not enable behavior analysis. See also Tables S3, S4, and Figure S3.

RESULTS AND DISCUSSION

The homologous series impacted larval behavior, only perfluorobutane sulfonamide impacted morphology

To investigate the developmental toxicity of the short-chain homologous series, embryonic zebrafish were exposed to a range of concentrations of each chemical (Table 1) and assessed for morphological and behavior endpoints at 24 and 120 h postfertilization (hpf). None of the PFAS exposures induced abnormal morphology at 24 hpf compared to controls. By 120 hpf, FBSA exposure induced a robust phenotypic response, with craniofacial abnormalities and edema being the most frequently occurring malformations, see Table S3 for lowest effect levels (LELs) and Table S4 for percent incidence of each endpoint. PFBS, PFPeA, or 4:2 FTS did not induce any significant morphological response. Considering the morphological response induced by FBSA exposure but not the remaining chemicals in the homologous series, it is evident that the sulfonamide head group imparted greater bioactivity, a trend also identified in other studies (Han et al., 2021; Dasgupta et al., 2020). To evaluate the totality of effects occurring in response

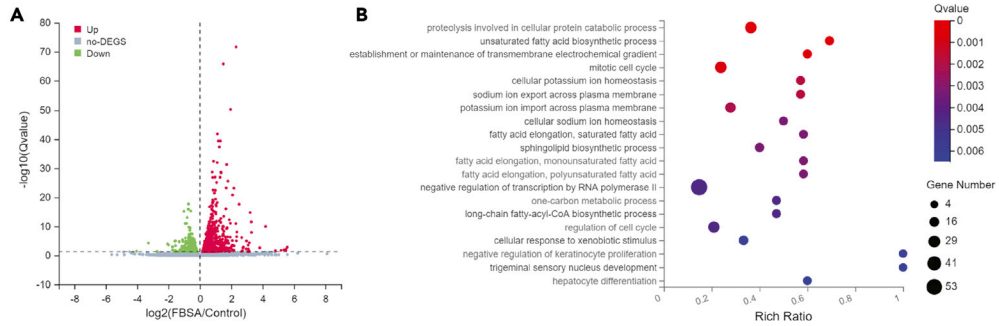

Figure 1. FBSA exposure significantly impacts gene expression at 48 hpf

(A) Volcano plot of differentially expressed transcripts. Red indicates upregulated differentially expressed genes, green indicates downregulated, and gray indicates that there was no differential expression.

(B) Gene Ontology- Enriched Biological Processes. The most significantly enriched biological processes (BP) are on the y axis (left). The x axis is the enrichment ratio (ratio of the number of genes within the present gene set that are annotated to a BP GO term over the total number of genes annotated to that BP GO term in the species. Size of dot bubble represents the number of DE-Gs annotated to a BP GO term. Color represents the significance of the enrichment: the redder the color, the smaller the q value. See also Table S5

to exposure, "any morphological effect" was used as a combination of all morphological effects observed during all assessments but was almost entirely driven by 120 hpf phenotypes in this study. FBSA exposure elicited an LEL for any morphological effect of 37 μM and reached 97% any effect for the 100 μM exposure group (Table 1). The modeled EC_{80} of FBSA using any morphological effect as the endpoint was 47 μM (Figure S2).

Similar to morphological endpoints, exposure to none of the PFAS elicited aberrant behavior measured by the embryonic photomotor response (EPR) assay at 24 hpf. However, all of the homologous series induced aberrant behavior in the larval photomotor response (LPR) assay at 120 hpf (Table 1; Figure S3 for LPR plots). FBSA was the most bioactive, eliciting a hypoactive LPR behavior in both the light and dark phases at the lowest concentration compared to the other chemicals in the series. At lower concentrations, 4:2 FTS exposure caused hyperactivity during the light phase, which shifted to hypoactivity at the two highest concentrations tested. Exposure to PFPeA induced hypoactivity during the light phase and hyperactivity during the dark phase of the assay, as previously published by Rericha et al. (2021). Lastly, PFBS exposure caused abnormal behavior in the light at the highest concentrations tested, hypoactivity at 43 μM and hyperactivity at 57 μM. Further analysis given this abrupt flip in activity revealed higher confidence in the hypoactivity call, as an LPR light period earlier in the assay also showed hypoactivity following 43 μM PFBS exposure. Developmental toxicity assessments revealed unique bioactivity profiles for each compound within this homologous series. To investigate whether global transcriptome-level changes could begin to explain differences in bioactivity profiles, we conducted a transcriptomic investigation with the homologous series.

Perfluorobutane sulfonamide exposure significantly impacts gene expression at 48 hpf

Conducting mRNA-seq at 48 hpf, our goal was to anchor our transcriptomic data to morphological phenotypes observed at 120 hpf and to interrogate transcriptional changes closer to toxic initiating events. Fish were sampled at 48 hpf, before any observable phenotypes, but at exposure concentrations where 80% of the fish would later manifest aberrant morphology at 120 hpf (only possible for FBSA). The same concentration of 47 μM was selected for all chemical exposures, and no overt morphological effects were yet noted at the time of sampling. FBSA was the only chemical that elicited substantial transcriptomic disruption with differential expression of 1,909 genes: 1,126 increased and 783 decreased (Figure 1A). The three other chemicals elicited only 14 misregulated genes (6 up and 8 down), 3 (2 up and 1 down), and 5 (all down) for PFPeA, 4:2 FTS, and PFBS, respectively. Our data on PFBS differed from a previous zebrafish-based study by Sant et al. The authors identified 438 differentially expressed genes (DE-Gs) in 4-day-old zebrafish following PFBS exposure at 32 μM (Sant et al., 2019), compared to the 5 we identified following exposure at 47 μM. Discrepancy between studies was likely owing to the differing sampling timepoint (4 days postfertilization by Sant et al. vs 48 hpf), exposure paradigms (1-4 days post fertilization exposures with daily renewal by Sant et al., vs 8-48 hpf static exposures), and zebrafish strains. The transcriptomic effects we

observed directly concurred with the morphological effects from our developmental toxicity assessments in that exposure to FBSA alone significantly perturbed normal development. Our findings demonstrate that PFAS functional head group is a robust predictor of toxicity and that significant exposure-induced changes in the transcriptome early in development preceded abnormal morphological development later. This study also illustrates that exposure to these compounds at concentrations leading to abnormal larval behavior, but not morphological effects at 120 hpf, may result in only a small number of differentially expressed transcripts, also reported by Shankar et al. for polycyclic aromatic hydrocarbons, another group of ubiquitous environmental contaminants (Shankar et al., 2019). To begin to elucidate the mechanisms by which these short-chain PFAS cause sub-lethal behavior effects, additional concentration and timepoint optimization specific to these endpoints will be necessary.

The present study, being the first to utilize mRNA-seq in zebrafish to explore transcriptome-level effects of FBSA, PFPeA, and 4:2 FTS, is an important step toward understanding mechanisms of toxicity and contribution of functional head groups. A significant strength of this study is establishing this consistent and highly controlled paradigm in a single model organism for the interrogation of mode of action of PFAS toxicity. Effects represented whole organism transcriptional changes, not specific to a certain tissue or cell type, and provided an unbiased snapshot of the entire transcriptome for the developing zebrafish following exposures. This dataset alone did not enable definitive identification of individual genes directly responsible for the initiation of toxic effects, as many diverse chemical exposures and perturbation of numerous biological pathways could lead to the manifestation of abnormal morphological endpoints. The capacity of the developmental zebrafish to detect chemical bioactivity occurring through such a variety of means is a significant strength of the model. With the present dataset, we were able to further explore transcriptomic effects using gene ontology and transcription factor analyses. Given the large transcriptional response following FBSA exposure, we focused on FBSA exposure-associated effects and the internal dose that led to them. Current findings combined with future transcriptomic investigations of additional PFAS using a consistent paradigm will be essential to tease apart key genes involved in the initiation of toxic effects and to prioritize genes for functional investigation.

Perfluorobutane sulfonamide-enriched biological pathways related to lipid metabolism and cellular homeostasis

Significantly enriched biological pathways in response to FBSA exposure were predominately related to metabolic processes involving lipid metabolism and biosynthesis (Figure 1B). Biological pathways involving fatty acid elongation and biosynthesis, as well as long-chain fatty-acyl-CoA biosynthesis and proteolysis, were disrupted. A significant disruption of lipid metabolism has also been shown in other studies of PFAS exposure using transcriptomics in zebrafish (Martinez et al., 2019) and mice (Roth et al., 2021), as well as proteomics and metabolomics in zebrafish (Shi et al., 2009; Gebreab et al., 2020) and mice (Tan et al., 2012; Yu et al., 2016), though these and other studies are overwhelmingly focused on long-chain legacy chemicals like PFOS and PFOA. The short-chain PFBS was also reported to disrupt lipid homeostasis in zebrafish by Sant et al. (2019). Several other biological pathways under the categories of developmental processes (brain and nervous system), biological regulation (ion homeostasis and transport), and immune system processes were also significantly enriched in the present study (Table S5). Many of the disrupted pathways could be implicated in the observed morphological and behavioral phenotypes, and future investigation will focus on individual genes of interest.

In addition to enriched biological pathways, we investigated transcription factor enrichment and identified 43 transcription factors that were differentially expressed within our FBSA exposure dataset (Table S6). Among these was Nuclear Factor erythroid-2 (NRF2), previously shown to be activated by various PFAS exposures in HepG2 cell assays (Houck et al., 2021) and to modulate embryonic zebrafish response to PFOS exposure (Sant et al., 2018). Our analysis also identified 191 enriched transcription factors predicted to regulate genes that were differentially expressed within our dataset. Most notably within this list is Peroxisome Proliferator-Activated Receptor alpha (PPARα), predicted to regulate 36 of the genes disrupted by FBSA exposure. PPARα has been widely associated with PFAS toxicity in the literature, specifically related to the dysfunction of lipid metabolism and liver processes (Fenton et al., 2021; Houck et al., 2021). Other transcription factors predicted to regulate FBSA-induced DE-Gs include Retinoid X Receptor alpha (RXRα, 56 DE-Gs) and Aryl Hydrocarbon Receptor (AHR, 54 DE-Gs). We plan to further investigate these insights into the mode of action of FBSA toxicity in future studies and to compare mRNA-seq data of additional compounds within our model.

Table 2. FBSA is the most bioaccumulative chemical in the series[a]

PFAS	Measured internal concentration (ng/mg)	BCF (L/kg)
FBSA	11 ± 1.5	0.80
PFBS	8.9 ± 0.99	0.63
4:2 FTS	3.3 ± 0.60	0.22
PFPeA	1.5 ± 0.15	0.12

[a]Analytically measured internal concentration (ng/mg tissue) at 48 hpf, and bioconcentration factor (BCF) following each chemical exposure at 47 μM.

Perfluorobutane sulfonamide is the most bioaccumulative chemical in the series

Given the differences in toxicity and gene expression changes across the 4-fluorinated carbon series, we investigated whether the variation could be completely explained by bioaccumulation. Analytical measurements of embryonic tissue concentration at 48 hpf were conducted following each chemical exposure at 47 μM. FBSA was the most bioaccumulative, with an internal concentration of 11 ± 1.5 ng/mg tissue (Table 2). PFBS exposure yielded a relatively similar body burden of 8.9 ± 0.99 ng/mg, while exposures to 4:2 FTS and PFPeA resulted in lower body burden of 3.3 ± 0.60 and 1.5 ± 0.15 ng/mg, respectively. Bioconcentration factors similarly illustrate differences between chemicals: FBSA (0.80) > PFBS (0.63) > 4:2 FTS (0.22) > PFPeA (0.12). The higher body burden of FBSA compared to the other chemicals of similar fluorinated chain length is likely owing to a larger percentage of FBSA in neutral charge at the pH of the embryo medium (7.3), enabling more favorable interactions with lipids and membranes (Nouhi et al., 2018). Utilizing an estimated pK_a of 6.2 for perfluorooctane sulfonamide (FOSA) (Rayne and Forest, 2009), the 8-fluorinated carbon homolog of FBSA, as a surrogate, the calculated fraction of FBSA in a neutral form in embryo media is 7% (Schwarzenbach et al., 2016). Conducting the equivalent calculation for PFBS and PFPeA, or their 8-fluorinated carbon counterparts, essentially 0% is in neutral form, with pK_a estimates that vary but are consistently reported as <3.8 (Vierke et al., 2013; Goss, 2008). High relative bioaccumulation of FOSA compared to other PFAS was also reported by Han et al. using developmental zebrafish (Han et al., 2021). Previous investigations into body burdens in developmental zebrafish identified similar trends: lower BCF for PFPeA than PFBS (Menger et al., 2019) and lower BCFs for perfluoroalkyl carboxylates than perfluoroalkyl sulfonates. These studies also reported much higher BCFs (>1,000) for PFOS, a long-chain legacy chemical (Menger et al., 2019; Gaballah et al., 2020). Although BCFs calculated for this homologous series do not implicate these compounds as bioaccumulative under regulatory framework (typically on the order of 2,000) (Schäfer et al., 2015), they provide important context for this investigation into toxicity.

Considering toxicity and transcriptomic changes with the context of body burden, 4:2 FTS and PFPeA exposures induced no morphological effects, only a small number of differentially expressed genes, and relatively low internal concentrations. If bioaccumulation was the sole driver of toxicity, we would expect high measured internal concentrations to be accompanied by a high incidence of developmental effects. Although this was true for FBSA, it was not the case for PFBS exposure, which caused a relatively high internal concentration but no teratogenicity and few genes with altered expression compared to controls. This study demonstrates that functional head group affects bioaccumulation, and furthermore, suggests that other functional head group-related factors, not just bioaccumulation, are influencing the bioactivity of these chemicals. Additional factors may include inherent capacity to interact with biological receptors, tissue-specific distribution, or metabolism. Sulfonamide PFAS, along with fluorotelomer sulfonic acids, have been shown to biotransform into terminal end products that include perfluoroalkyl carboxylates and sulfonates (Buck et al., 2011). Although metabolism was not addressed in this study, the toxicity of parent compounds can inform the prioritization of compounds for future investigations. Interrogating the body burden of a homologous series of short-chain PFAS in combination with toxicological and transcriptomic endpoints provided a more holistic understanding of their effects on development.

In summary, across the 4-fluorinated carbon PFAS series, all chemicals induced larval behavior effects, but only FBSA caused morphological, behavioral, and large-scale transcriptomic disruptions. Notably, exposures at concentrations shown to induce only behavior effects resulted in a small number of differentially expressed genes, suggesting further optimization of concentration and timepoint are needed to investigate mechanisms of this sub-teratogenic toxicity. Biological processes enriched following FBSA exposure

were related to lipid metabolism and biosynthesis, cellular homeostasis, brain and nervous system development, and immune processes. The bioaccumulative potential of the series was FBSA > PFBS >4:2 FTS > PFPeA; BCFs did not classify these chemicals as bioaccumulative within regulatory frameworks but provided insight into toxicity. High FBSA and low PFPeA and 4:2 FTS tissue concentrations were in concordance with high and low morphological and transcriptional effects, respectively. However, the relatively high tissue concentration of PFBS but low bioactivity suggested there may be additional factors of toxicity at play, beyond bioaccumulation, and further investigation is warranted. Collectively, this study demonstrated that PFAS functional head group is a driver of developmental toxicity. We hope future studies will emulate our approach, leveraging the throughput of the developmental zebrafish to rapidly expand knowledge of the hazards that additional structural classes might present.

Limitations of the study

This study provides a structurally guided *in vivo* comparison of the developmental toxicity of a short-chain series supported by transcriptomics and analytical body burden measurements. Using developmental zebrafish, we investigated endpoints at the organismal level and therefore cannot draw conclusions about the specific cell or tissue types. Although our top-down approach has this limitation, it is well-suited for evaluating the overall hazard and bioactivity of chemicals and generating informed hypotheses for future investigation. Current results pose the question of whether PFAS with equivalent body burden would elicit similar developmental toxicity. This study did not measure body burden at the EC_{80} for each chemical in the homologous series as abnormal morphology was not observed for three of the chemicals within the reasonable nominal concentration range. Future work to anchor internal concentration and directly compare chemical bioactivity would provide additional clarity on the importance of bioaccumulation for the toxicity of this chemical class. Another limitation to consider is the use of adjusted nominal exposure concentration instead of measured exposure concentration in the calculation of BCFs. The analytical validation of stock concentration we conducted was essential, and additional measurements of exposure solution could provide additional insight into short-chain PFAS partitioning. Lastly, the fact that only one chemical induced significant transcriptional effects at the evaluated timepoint and concentration did not allow for the comparison of multiple compounds within our model system. Future work will assess the transcriptome-wide impact of additional structurally diverse PFAS to facilitate such comparisons.

STAR★METHODS

Detailed methods are provided in the online version of this paper and include the following:

- KEY RESOURCES TABLE
- RESOURCE AVAILABILITY
  - Lead contact
  - Material availability
  - Data and code availability
- EXPERIMENTAL MODEL AND SUBJECT DETAILS
  - Zebrafish husbandry
- METHODS DETAILS
  - Chemicals and preparation of stock solutions
  - Chemical exposure
  - Developmental toxicity testing
  - RNA sample collections and homogenizations
  - RNA isolation and sequencing
  - Analysis of mRNA-seq data
  - Embryonic body burden

SUPPLEMENTAL INFORMATION

Supplemental information can be found online at https://doi.org/10.1016/j.isci.2022.103789.

ACKNOWLEDGMENTS

The authors would like to acknowledge the staff at the Sinnhuber Aquatic Research Laboratory who made this research possible. This research was funded by the United States Environmental Protection Agency,

grant number 83948101, the National Institute of Health and Sciences, grant number P30 ES030287, and the T32 Integrated Regional Training Program in Environmental Health Sciences, grant number T32 ES007060.

AUTHOR CONTRIBUTIONS

Conceptualization, R.T. and Y.R.; methodology, Y.R., D.P., L.T., and R.T.; software and data curation, L.T.; validation, Y.R.; formal analysis, Y.R., D.P., and L.T.; investigation, Y.R and D.P.; resources, J.A. and R.T.; writing—original draft preparation, Y.R.; writing—review and editing, M.S., L.T., D.P., J.A., and R.T.; visualization, Y.R.; project administration, Y.R.; supervision and funding acquisition, L.T, J.A., and R.T. All authors have read and agreed to the published version of the manuscript.

DECLARATION OF INTERESTS

The authors declare no competing interests.

Received: October 21, 2021
Revised: December 23, 2021
Accepted: January 13, 2022
Published: February 18, 2022

REFERENCES

Ateia, M., Maroli, A., Tharayil, N., and Karanfil, T. (2019). The overlooked short- and ultrashort-chain poly- and perfluorinated substances: a review. Chemosphere *220*, 866–882.

Barton, C.L., Johnson, E.W., and Tanguay, R.L. (2016). Facility design and health management program at the sinnhuber aquatic research laboratory. Zebrafish *13*, S39–S43.

Blum, A., Balan, S.A., Scheringer, M., Trier, X., Goldenman, G., Cousins, I.T., Diamond, M., Fletcher, T., Higgins, C., Lindeman, A.E., et al. (2015). The madrid statement on poly- and perfluoroalkyl substances (PFASs). Environ. Health Perspect. *123*, A107–A111.

Brendel, S., Fetter, E., Staude, C., Vierke, L., and Biegel-Engler, A. (2018). Short-chain perfluoroalkyl acids: environmental concerns and a regulatory strategy under REACH. Environ. Sci. Eur. *30*, 9.

Buck, R.C., Franklin, J., Berger, U., Conder, J.M., Cousins, I.T., De Voogt, P., Jensen, A.A., Kannan, K., Mabury, S.A., and Van Leeuwen, S.P. (2011). Perfluoroalkyl and polyfluoroalkyl substances in the environment: terminology, classification, and origins. Integr. Environ. Assess. Manag. *7*, 513–541.

Cai, D., Li, Q.Q., Chu, C., Wang, S.Z., Tang, Y.T., Appleton, A.A., Qiu, R.L., Yang, B.Y., Hu, L.W., Dong, G.H., and Zeng, X.W. (2020). High transplacental transfer of perfluoroalkyl substances alternatives in the matched maternal-cord blood serum: evidence from a birth cohort study. Sci. Total Environ. *705*, 135885.

Chu, S., Letcher, R.J., Mcgoldrick, D.J., and Backus, S.M. (2016). A new fluorinated surfactant contaminant in biota: perfluorobutane sulfonamide in several fish species. Environ. Sci. Technol. *50*, 669–675.

Dasgupta, S., Dunham, C.L., Truong, L., Simonich, M.T., Sullivan, C.M., and Tanguay, R.L. (2021). Phenotypically anchored mRNA and miRNA expression profiling in zebrafish reveals flame retardant chemical toxicity networks. Front. Cell Dev. Biol. *9*, 663032.

Dasgupta, S., Reddam, A., Liu, Z., Liu, J., and Volz, D.C. (2020). High-content screening in zebrafish identifies perfluorooctanesulfonamide as a potent developmental toxicant. Environ. Pollut. *256*, 113550.

Davis, A.P., Grondin, C.J., Johnson, R.J., Sciaky, D., Wiegers, J., Wiegers, T.C., and Mattingly, C.J. (2021). Comparative Toxicogenomics Database (CTD): update 2021. Nucleic Acids Res. *49*, D1138–D1143.

Fenton, S.E., Ducatman, A., Boobis, A., Dewitt, J.C., Lau, C., Ng, C., Smith, J.S., and Roberts, S.M. (2021). Per- and polyfluoroalkyl substance toxicity and human health review: current state of knowledge and strategies for informing future research. Environ. Toxicol. Chem. *40*, 606–630.

Gaballah, S., Swank, A., Sobus, J.R., Howey, X.M., Schmid, J., Catron, T., Mccord, J., Hines, E., Strynar, M., and Tal, T. (2020). Evaluation of developmental toxicity, developmental neurotoxicity, and tissue dose in zebrafish exposed to GenX and other PFAS. Environ. Health Perspect. *128*, 47005.

Gao, K., Zhuang, T., Liu, X., Fu, J., Zhang, J., Fu, J., Wang, L., Zhang, A., Liang, Y., Song, M., and Jiang, G. (2019). Prenatal exposure to per- and polyfluoroalkyl substances (PFASs) and association between the placental transfer efficiencies and dissociation constant of serum proteins-PFAS complexes. Environ. Sci. Technol. *53*, 6529–6538.

Gebreab, K.Y., Eeza, M.N.H., Bai, T., Zuberi, Z., Matysik, J., O'shea, K.E., Alia, A., and Berry, J.P. (2020). Comparative toxicometabolomics of perfluorooctanoic acid (PFOA) and next-generation perfluoroalkyl substances. Environ. Pollut. *265*, 114928.

Geier, M.C., Chlebowski, A.C., Truong, L., Massey Simonich, S.L., Anderson, K.A., and Tanguay, R.L. (2018). Comparative developmental toxicity of a comprehensive suite of polycyclic aromatic hydrocarbons. Arch. Toxicol. *92*, 571–586.

Gluge, J., Scheringer, M., Cousins, I.T., Dewitt, J.C., Goldenman, G., Herzke, D., Lohmann, R., NG, C.A., Trier, X., and Wang, Z. (2020). An overview of the uses of per- and polyfluoroalkyl substances (PFAS). Environ. Sci. Process. Impacts *22*, 2345–2373.

Goss, K.-U. (2008). The pKa values of PFOA and other highly fluorinated carboxylic acids. Environ. Sci. Technol. *42*, 456–458.

Han, J., Gu, W., Barrett, H., Yang, D., Tang, S., Sun, J., Liu, J., Krause, H.M., Houck, K.A., and Peng, H. (2021). A roadmap to the structure-related metabolism pathways of per- and polyfluoroalkyl substances in the early life stages of zebrafish (*Danio rerio*). Environ. Health Perspect. *129*, 77004.

Horzmann, K.A., and Freeman, J.L. (2018). Making waves: new developments in toxicology with the zebrafish. Toxicol. Sci. *163*, 5–12.

Houck, K.A., Patlewicz, G., Richard, A.M., Williams, A.J., Shobair, M.A., Smeltz, M., Clifton, M.S., Wetmore, B., Medvedev, A., and Makarov, S. (2021). Bioactivity profiling of per- and polyfluoroalkyl substances (PFAS) identifies potential toxicity pathways related to molecular structure. Toxicology *457*, 152789.

Howe, K., Clark, M.D., Torroja, C.F., Torrance, J., Berthelot, C., Muffato, M., Collins, J.E., Humphray, S., Mclaren, K., Matthews, L., et al. (2013). The zebrafish reference genome sequence and its relationship to the human genome. Nature *496*, 498–503.

Li, F., Duan, J., Tian, S., Ji, H., Zhu, Y., Wei, Z., and ZhaO, D. (2019). Short-chain per- and polyfluoroalkyl substances in aquatic systems:

occurrence, impacts and treatment. Chem. Eng. J. *380*, 122506.

Li, X., Fatowe, M., Cui, D., and Quinete, N. (2022). Assessment of per- and polyfluoroalkyl substances in Biscayne Bay surface waters and tap waters from South Florida. Sci. Total Environ. *806*, 150393.

Mandrell, D., Truong, L., Jephson, C., Sarker, M.R., Moore, A., Lang, C., Simonich, M.T., and Tanguay, R.L. (2012). Automated zebrafish chorion removal and single embryo placement: optimizing throughput of zebrafish developmental toxicity screens. J. Lab Autom. *17*, 66–74.

Martinez, R., Navarro-Martin, L., Luccarelli, C., Codina, A.E., Raldua, D., Barata, C., Tauler, R., and Pina, B. (2019). Unravelling the mechanisms of PFOS toxicity by combining morphological and transcriptomic analyses in zebrafish embryos. Sci. Total Environ. *674*, 462–471.

Menger, F., Pohl, J., Ahrens, L., Carlsson, G., and Orn, S. (2019). Behavioural effects and bioconcentration of per- and polyfluoroalkyl substances (PFASs) in zebrafish (*Danio rerio*) embryos. Chemosphere *245*, 125573.

Nouhi, S., Ahrens, L., Pereira, H.C., Hughes, A.V., Campana, M., Gutfreund, P., Palsson, G.K., Vorobiev, A., and Hellsing, M.S. (2018). Interactions of perfluoroalkyl substances with a phospholipid bilayer studied by neutron reflectometry. J. Colloid Interf. Sci. *511*, 474–481.

Padilla, S., Corum, D., Padnos, B., Hunter, D.L., Beam, A., Houck, K.A., Sipes, N., Kleinstreuer, N., Knudsen, T., Dix, D.J., and Reif, D.M. (2012). Zebrafish developmental screening of the ToxCast Phase I chemical library. Reprod. Toxicol. *33*, 174–187.

Qian, X., Ba, Y., Zhuang, Q., and Zhong, G. (2014). RNA-Seq technology and its application in fish transcriptomics. OMICS *18*, 98–110.

Rayne, S., and Forest, K. (2009). Comment on "indirect photolysis of perfluorochemicals: hydroxyl radical-initiated oxidation of N -ethyl perfluorooctane sulfonamido acetate (N -EtFOSAA) and other perfluoroalkanesulfonamides". Environ. Sci. Technol. *43*, 7995–7996.

Reif, D.M., Truong, L., Mandrell, D., Marvel, S., Zhang, G., and Tanguay, R.L. (2016). High-throughput characterization of chemical-associated embryonic behavioral changes predicts teratogenic outcomes. Arch. Toxicol. *90*, 1459–1470.

Rericha, Y., Cao, D., Truong, L., Simonich, M., Field, J.A., and Tanguay, R.L. (2021). Behavior effects of structurally diverse per- and polyfluoroalkyl substances in zebrafish. Chem. Res. Toxicol. *34*, 1409–1416.

Roth, K., Yang, Z., Agarwal, M., Liu, W., Peng, Z., Long, Z., Birbeck, J., Westrick, J., Liu, W., and Petriello, M.C. (2021). Exposure to a mixture of legacy, alternative, and replacement per- and polyfluoroalkyl substances (PFAS) results in sex-dependent modulation of cholesterol metabolism and liver injury. Environ. Int. *157*, 106843.

Saili, K.S., Corvi, M.M., Weber, D.N., Patel, A.U., Das, S.R., Przybyla, J., Anderson, K.A., and Tanguay, R.L. (2012). Neurodevelopmental low-dose bisphenol A exposure leads to early life-stage hyperactivity and learning deficits in adult zebrafish. Toxicology *291*, 83–92.

Sant, K.E., Sinno, P.P., Jacobs, H.M., and Timme-Laragy, A.R. (2018). Nrf2a modulates the embryonic antioxidant response to perfluorooctanesulfonic acid (PFOS) in the zebrafish, Danio rerio. Aquat. Toxicol. *198*, 92–102.

Sant, K.E., Venezia, O.L., Sinno, P.P., and Timme-Laragy, A.R. (2019). Perfluorobutanesulfonic acid disrupts pancreatic organogenesis and regulation of lipid metabolism in the zebrafish, Danio rerio. Toxicol. Sci. *167*, 258–268.

Schäfer, S., Buchmeier, G., Claus, E., Duester, L., Heininger, P., Körner, A., Mayer, P., Paschke, A., Rauert, C., Reifferscheid, G., et al. (2015). Bioaccumulation in aquatic systems: methodological approaches, monitoring and assessment. Environ. Sci. Eur. *27*, 5.

Schwarzenbach, R.P., Gschwend, P.M., and Imboden, D.M. (2016). Environmental Organic Chemistry (John Wiley & Sons).

Shankar, P., Geier, M.C., Truong, L., Mcclure, R.S., Pande, P., Waters, K.M., and Tanguay, R.L. (2019). Coupling genome-wide transcriptomics and developmental toxicity profiles in zebrafish to characterize polycyclic aromatic hydrocarbon (PAH) hazard. Int. J. Mol. Sci. *20*, 2570.

Shankar, P., Mcclure, R.S., Waters, K.M., and Tanguay, R.L. (2021). Gene co-expression network analysis in zebrafish reveals chemical class specific modules. BMC Genomics *22*, 658.

Shi, X., Yeung, L.W.Y., Lam, P.K.S., Wu, R.S.S., and Zhou, B. (2009). Protein profiles in zebrafish (*Danio rerio*) embryos exposed to perfluorooctane sulfonate. Toxicol. Sci. *110*, 334–340.

Tan, F., Jin, Y., Liu, W., Quan, X., Chen, J., and Liang, Z. (2012). Global liver proteome analysis using iTRAQ labeling quantitative proteomic technology to reveal biomarkers in mice exposed to perfluorooctane sulfonate (PFOS). Environ. Sci. Technol. *46*, 12170–12177.

Tilton, S.C., Tal, T.L., Scroggins, S.M., Franzosa, J.A., Peterson, E.S., Tanguay, R.L., and Waters, K.M. (2012). Bioinformatics Resource Manager v2.3: an integrated software environment for systems biology with microRNA and cross-species analysis tools. BMC Bioinformatics *13*, 311.

Truong, L., Bugel, S.M., Chlebowski, A., Usenko, C.Y., Simonich, M.T., Simonich, S.L., and Tanguay, R.L. (2016). Optimizing multi-dimensional high throughput screening using zebrafish. Reprod. Toxicol. *65*, 139–147.

Truong, L., Harper, S.L., and Tanguay, R.L. (2011). Evaluation of embryotoxicity using the zebrafish model. Methods Mol. Biol. *691*, 271–279.

Truong, L., Marvel, S., Reif, D.M., Thomas, D., Pande, P., Dasgupta, S., Simonich, M.T., Waters, K.M., and Tanguay, R.L. (2020). The multi-dimensional embryonic zebrafish platform predicts flame retardant bioactivity. Reprod. Toxicol. *96*, 359–369.

Truong, L., Reif, D.M., St Mary, L., Geier, M.C., Truong, H.D., and Tanguay, R.L. (2014). Multidimensional in vivo hazard assessment using zebrafish. Toxicol. Sci. *137*, 212–233.

Truong, L., Saili, K.S., Miller, J.M., Hutchison, J.E., and Tanguay, R.L. (2012). Persistent adult zebrafish behavioral deficits results from acute embryonic exposure to gold nanoparticles. Comp. Biochem. Physiol. C Toxicol. Pharmacol. *155*, 269–274.

Vierke, L., Berger, U., and Cousins, I.T. (2013). Estimation of the acid dissociation constant of perfluoroalkyl carboxylic acids through an experimental investigation of their water-to-air transport. Environ. Sci. Technol. *47*, 11032–11039.

Wang, Z.Y., Dewitt, J.C., Higgins, C.P., and Cousins, I.T. (2017). A never-ending story of per- and polyfluoroalkyl substances (PFASs)? Environ. Sci. Technol. *51*, 2508–2518.

Westerfield, M. (2000). The Zebrafish Book: A Guide for the Laboratory Use of Zebrafish (Danio rerio), 4th (University of Oregon).

Yao, X., Cao, D., Wang, F., Zhang, W., Ma, C., and Song, M. (2019). An overview of omics approaches to characterize the effect of perfluoroalkyl substances in environmental health. Trac Trends Anal. Chem. *121*, 115367.

Yu, N.Y., Wei, S., Li, M.Y., Yang, J.P., Li, K., Jin, L., Xie, Y.W., Giesy, J.P., Zhang, X.W., and Yu, H.X. (2016). Effects of perfluorooctanoic acid on metabolic profiles in brain and liver of mouse revealed by a high-throughput targeted metabolomics approach. Sci. Rep. *6*, 23963.

Zhang, G., Truong, L., Tanguay, R.L., and Reif, D.M. (2017). A new statistical approach to characterize chemical-elicited behavioral effects in high-throughput studies using zebrafish. PLoS One *12*, e0169408.

STAR★METHODS

KEY RESOURCES TABLE

REAGENT or RESOURCE	SOURCE	IDENTIFIER
Chemicals, peptides, and recombinant proteins		
Potassium nonafluoro-1-butanesulfonate (PFBS)	Sigma Aldrich	Cat#294209
n-Perfluoropentanoic acid (PFPeA)	Matrix Scientific	Cat#006057
Perfluorobutylsulfonamide (FBSA)	Synquest Laboratories	Cat#8169-3-07
1H,1H,2H,2H-Perfluorohexanesulfonic acid (4:2 FTS)	Synquest Laboratories	Cat#6164-3-38
Methanol	Fisher Scientific	Cat#A456-500
RNAzol RT	Molecular Research Center	Cat#RN190
Acetonitrile	Fisher Scientific	Cat#A998-4
Critical commercial assays		
Direct-zol RNA MiniPrep kit	Zymo Research	Cat#R2052
BGISEQ-500 sequencing platform	Beijing Gemonics Institute	https://www.bgi.com/global/home
Deposited data		
mRNA-seq data	This paper	GEO: GSE186576
Developmental toxicity data	This paper (Data S1)	N/A
Experimental models: Organisms/strains		
Danio rerio (zebrafish)	See experimental model and subject details section	N/A
Software and algorithms		
ZebraBox	ViewPoint Behavior Technology	https://www.viewpoint.fr/en/home
Dr. Tom Data Visualization Solution	Beijing Genomics Institute	https://www.bgi.com/global/dr-tom/
Bioinformatics Resource Manager	Tilton et al., 2012	https://cbb.pnnl.gov/brm/
GeneGo Metacore	Clarivate	https://portal.genego.com/
Other		
Falcon 96-well plates	Corning	Cat#353227
Sealing film	VWR	Cat#89134-428
Bullet Blender Tissue Homogenizer	Next Advance	https://www.nextadvance.com/bullet-blender-homogenizer/
Agilent 1100 series HPLC	Agilent Technologies	https://www.agilent.com/en/product/liquid-chromatography
Waters Acquity triple quadrupole mass spectrometer	Waters Corporation	https://www.waters.com/nextgen/us/en.html
Zorbax Eclipse Plus C18, 4.6 × 75 mm × 3.5 μm	Agilent Technologies	Cat#959933-902
Zorbax Eclipse Plus C18, 4.6 × 50 mm × 5 μm	Agilent Technologies	Cat#959946-902
Supelclean ENVI-Carb SPE Bulk Packing	Sigma Aldrich	Cat#57210-U

RESOURCE AVAILABILITY

Lead contact

Requests for further information or resources should be directed to and will be fulfilled by the lead contact, Dr. Robyn L. Tanguay (robyn.tanguay@oregonstate.edu).

Material availability

This study did not generate new unique reagents.

Data and code availability

mRNA-seq data have been deposited at GEO and are publicly available as of November 2021. The accession number is listed in the key resources table. Raw data for all developmental toxicity assessments can be found in Data S1, with a raw data guide available in Data S2. This paper does not report original code. Any additional information required to reanalyze the data reported in this paper is available from the lead contact upon request.

EXPERIMENTAL MODEL AND SUBJECT DETAILS

Zebrafish husbandry

Zebrafish (tropical 5D wild type) were spawned and housed at the Sinnhuber Aquatic Research Laboratory (SARL), Oregon State University (Corvallis, OR, USA), in a specific pathogen-free (SPF) colony. All husbandry and experimental protocols were approved by the Institutional Animal Care and Use Committee (Oregon State Univ. IACUC-2021-0166 and ACUP# 5113) (Barton et al., 2016). Brood stock were maintained at 400 fish/50 gallon tank densities in recirculating 28 ± 1°C filtered water supplemented with Instant Ocean salts (Spectrum Brands, Blacksburg, VA) and sodium bicarbonate to achieve a pH of 7.4, with a 14:10 h light:dark cycle. Spawning funnels placed in the tanks at night facilitated spawning and embryo collections the following morning. Embryos were staged and maintained at 28°C in embryo medium (EM) consisting of 15 mM NaCl, 0.5 mM KCl, 1 mM $MgSO_4$, 0.15 mM KH_2PO_4, 0.05 mM NA_2HPO_4, and 0.7 mM $NaHCO_3$ (Westerfield, 2000).

METHODS DETAILS

Chemicals and preparation of stock solutions

The homologous series consisted of perfluorobutane sulfonate (PFBS), perfluoropentanoic acid (PFPeA), perfluorobutane sulfonamide (FBSA), and 1H,1H,2H,2H-perfluorohexanesulfonic acid (4:2 FTS) (see Table S1 for additional manufacturer details and Figure S1 for chemical structures). Stock solutions of PFBS, FBSA, and 4:2 FTS were prepared by weighing 0.080–0.1030 g solid on an analytical scale and dissolving the mass into 15 mL polypropylene (PPE) bottles using 15 mL LC/MS grade methanol (CAS: 67-56-1) to achieve a nominal stock concentration of 22 mM. For the PFPeA, which was obtained as a liquid, 60–80 mL were added to a 30 mL PPE bottle and 25 mL methanol was added. Methanol, previously used to investigate PFAS toxicity in zebrafish (Rericha et al. 2021), was an effective solvent for 22–30 mM stock solutions and enabled streamlined analytical validation of stock concentrations, without need for solvent exchange. Chemical stocks were shaken on an orbital shaker overnight. For analytical validation, one aliquot of each stock solution was diluted with methanol and spiked with 0.75 ng mass-labelled standards (Data S3). Samples were measured using high-performance liquid chromatography and triple quadrupole mass spectrometry (LC-MS/MS), specifically using an Agilent 1100 series High Pressure Liquid Chromatograph (Santa Clara, CA), a Waters Acquity Triple Quadrupole Mass Spectrometer (Milford, MA), and the configuration described in Rericha et al. (2021). Analytically measured stock concentrations were then used to calculate adjusted exposure concentrations (from nominal exposure concentrations that ranged from 1-100 μM) throughout this study:

PFAS	CAS	Nominal Stock Concentration (mM)	Measured Stock Concentration (mM)	Adjusted Exposure Concentrations for Developmental Toxicity Testing (μM)
PFBS	29420-49-3	22	13	0.60, 1.4, 3.7, 9.3, 20, 43, 57
PFPeA	2706-90-3	30	15	0.70, 1.7, 4.4, 11, 24, 52, 69
FBSA	30334-69-1	22	23	1.0, 2.7, 6.8, 17, 37, 78, 100
4:2 FTS	757124-72-4	22	19	0.9, 2.2, 5.5, 14, 30, 64, 85

Chemical exposure

Embryos were dechorionated at 4 hours postfertilization (hpf) using pronase and a custom automated system and placed in 96-well plates (Falcon®, product number: 353227) that were prefilled with 100 μL EM, 1

embryo per well (Mandrell et al., 2012). Following embryo placement, 50 μL EM was removed from each well. Embryos then underwent either vehicle control exposure (0.5% methanol) or individual chemical exposures (normalized to 0.5% methanol) at 8 hpf (n = 36). In a previous study, we identified 0.5% methanol as an acceptable concentration to which developing zebrafish were tolerant, with no significant effects on morphology or behavior endpoints (Rericha et al., 2021). The target range of nominal exposure concentrations was 1–100 μM, a broad range in which to detect chemical bioactivity, which was then adjusted post-testing to account for analytically measured stock solution concentrations. To achieve the desired nominal exposure concentrations, chemical stocks in 100% methanol underwent a series of serial dilutions in methanol, a 100x dilution in EM to achieve a 1% methanol working solution, and then a final 2x dilution as 50 μL working solution was added to each well (Rericha et al., 2021). Following exposure, plates were pressure/heat sealed (VWR Cat No. 89134-428) to minimize evaporation, shaken overnight on an orbital shaker at 235 rpm. Static exposure continued without shaking, maintaining fish in the dark at 28°C, until developmental toxicity assessments or sampling.

Developmental toxicity testing

Embryos were exposed to nominal PFAS concentrations of 0, 1.0, 2.5, 6.5, 16, 35, 75, and 100 μM. Reported exposure concentration throughout the rest of this study were adjusted for measured stock concentrations. Behavior and morphology assessments were conducted at both 24 and 120 hpf, following standard protocols highly suited for high-throughput chemical screening and extensively utilized by previous studies (Truong et al., 2014, 2020; Geier et al., 2018).

At 24 hpf, after embryos had been maintained in darkness overnight, behavior was assessed using an embryonic photomotor response (EPR) assay (Reif et al., 2016). The assay consisted of 30 s of darkness (IR) considered as the background period, a 1 s pulse of visible light (13,500 lux) followed by 9 s darkness as the excitation period, and then another pulse of visible light followed by 10 s darkness as the refractory period. Photomotor response in the form of spontaneous tail contractions was recorded using a custom Photomotor Response Analysis Tool (PRAT). Data corresponding to dead or delayed embryos were removed prior to data analysis; total movement of treated embryos was compared to that of controls using a Kolmogorov-Smirnov (K-S) test (Bonferroni-corrected p-value 0.05) (Reif et al., 2016). Following this 24 hpf behavior assessment, 3 morphological endpoints were assessed: mortality, delayed development, and spontaneous movement (Truong et al., 2016).

At 120 hpf, photomotor behavior was assessed using a larval photomotor response (LPR) assay. During this 24 minute assay, fish underwent 4 cycles of alternating 3 min light (900 lux) and 3 min dark (IR) periods; Zebraboxes (Viewpoint Behavior Technologies) tracked each larvae's movement, integrating over 6 s time bins (Saili et al., 2012; Truong et al., 2012). The first 3 cycles were treated as an acclimation period, and the 4th cycle was analyzed (Rericha et al., 2021). Data from dead or malformed fish were removed, and at least 70% of the original exposure group was required to be phenotypically normal prior to data analysis, which consisted of plotting total distance moved and modelling differential entropy. Statistical differences between exposure groups and controls were calculated using area under the curve ratios and a K-S test (Zhang et al., 2017). 10 morphological endpoints were also assessed at 120 hpf, including mortality (see Table S2A for endpoint descriptions and Table S2B for additional endpoint information) (Truong et al., 2011). Collection of all developmental toxicity data was blinded prior to analysis.

RNA sample collections and homogenizations

To phenotypically anchor transcriptional changes to morphology endpoints and to ensure a robust gene expression response, we aimed to conduct exposures at concentrations that caused approximately 80% incidence of any morphological effect (EC_{80}) at 120 hpf. The EC_{80} for each chemical was estimated by fitting mean percent incidence of any morphological effect using a Hill Model four-parameter log-logistic function and the drm function from the drc package in R (Shankar et al., 2019). Due to a lack of significant phenotypic responses to PFBS, PFPeA, and 4:2 FTS exposures, EC_{80}'s were unattainable. Therefore, the FBSA EC_{80} of 47 μM was used for all chemical exposure groups. We collected samples for RNA-seq at 48 hpf, before observable morphological effects occurred. This sampling timepoint enabled investigation of exposure effects on the transcriptomic landscape closer to toxic molecular initiating events. Additionally, 48 hpf has been extensively utilized in this context by our laboratory for a broad variety of chemicals and paired with the high throughput screening platform (Shankar et al., 2019, 2021; Dasgupta et al., 2021). Maintaining this consistent protocol enables effective comparison of transcriptomic data across datasets.

Following the above-described exposure paradigm, 4 replicates of 10 pooled zebrafish per exposure group were collected at 48 hpf, including a solvent control group. Zebrafish were euthanized on ice, excess water was removed, and samples were homogenized in 1.5 mL safe-lock tubes (Eppendorf, Enfield, CT) with 200 μL RNAzol (Molecular Research Center, Cincinnati, OH) and 0.5 mm zirconium oxide beads using a Bullet Blender (Next Advance, Averill Park, NY) for 3 minutes at speed 8. An additional 300 μL RNAzol was added, and homogenates were stored at −80°C until RNA isolation. Following sampling at the 48 hpf timepoint before visible morphological effects, holdback plates, which were additional plates treated identically to the sampling plates but maintained until 120 hpf, were used to confirm that the acceptable range of 70–100% any morphological effect was achieved (n = 48). While the effect percentages were not identical between all subsections of this study, those for FBSA consistently fell within the acceptable range, and all others were consistently below 30%.

RNA isolation and sequencing

Total RNA was isolated using a Direct-zol RNA MiniPrep kit (Zymo, Irvine, CA), including a DNase I digestion step. RNA quality was validated using the Agilent Bioanalyzer 2100 at the Center for Quantitative Life Sciences at Oregon State University (RIN >9). RNA-seq library preparation and sequencing were conducted by Beijing Genomics Institute (BGI; ShenZhen, China) using the BGISEQ-500 platform. Briefly, mRNA was purified using oligo(dT)-attached magnetic beads and fragmented, cDNA was synthesized, subjected to end-repair and 3′ adenylated, adapters were ligated to cDNA fragments, and then fragments were amplified and purified. Library quality was validated using an Agilent Technologies 2100 bioanalyzer. PCR products were denatured, circularized and formatted into the final library. The library was amplified with phi29 to form DNA nanoball, loaded into the patterned nanoarray, and sequenced using the BGISEQ-500.

Analysis of mRNA-seq data

Data analysis and visualization was also conducted by BGI and their Dr. Tom platform (https://www.bgi.com/global/dr-tom/). Briefly, SOAPnukes (v1.5.2) was used to filter sequencing data: reads with adapter sequences, low-quality base ratios >20%, or unknown base ratios >5% were removed. Clean read FASTQ files were mapped to the *Danio rerio* GRCz11 genome using HISAT2 (v2.0.4). Gene fusions and differential splicing were detected using Ericscript (v0.5.5) and rMATS (v3.2.5), respectively, clean read alignment conducted using Bowtie2 (v2.2.5), and expression levels were calculated using RSEM (v1.2.12). Differential expression analysis was performed using DESeq2 (Q-value $\leq$ 0.05), followed by gene ontology (GO) enrichment using Phyper based on Hypergeometric test (Q-value $\leq$ 0.05; Bonferroni). Transcription factor enrichment analysis was performed by first converting differentially expressed genes to their human orthologues using the Bioinformatics Resource Manager (BRM) (Tilton et al., 2012), followed by analysis using GeneGo Metacore software (https://portal.genego.com/).

Embryonic body burden

To quantify internal PFAS concentration at the mRNA-seq sampling timepoint, the same exposure paradigm and concentrations as for mRNA-seq samples were used. Once again, holdback plates were used to confirm that chemical exposures resulted in expected any morphological effect percentages. Washing of zebrafish within the 96-well plates to remove external chemical immediately prior to sampling consisted of an initial removal of 50 μL exposure solution followed by 11 rounds of adding 250 μL EM and removing 250 μL, sufficiently diluting exposure solutions to 2 orders of magnitude below the analytical limit of detection. At 48 hpf, 4 replicates of 40 pooled zebrafish per exposure group were collected. Samples were homogenized in 200 μL acetonitrile (CAS: 75-05-8) with 0.5 mm stainless steel beads using a Bullet Blender (Next Advance, Troy, NY) for 6 minutes at speed 8, and stored at −80°C until further processing.

To extract the embryonic zebrafish samples, homogenate was transferred into 15 mL PPE centrifuge tubes and the original container was thrice rinsed with 1 mL acetonitrile. Samples were spiked with 30 μL surrogate standard (Data S3), vortexed vigorously, then let sit for at least 30 min. 3 mL acetonitrile was added, followed by vortexing, sonication for 10 min, and centrifugation for 5 min at 5,000 RPM. Liquid was decanted into a new 15 mL centrifuge tube, 3 mL acetonitrile was added, and then this process was repeated. Following subsequent addition of 30 μL ethylene glycol, samples were evaporated and reconstituted with 3 mL methanol. Samples were added to a 100 mg Bulk Envi-carb, vortexed for at least 10 seconds, and centrifuged for 5 min at 5,000 RPM. Liquid was decanted into a new 15 mL centrifuge tube. 3 mL methanol was added to the tube with an Envi-Carb column. Liquid was decanted, sample was evaporated, and then

reconstituted to 150 μL final extract volume. 50 μL aliquots of the extract were then diluted with 40 μL methanol, 50 μL NaCl solution (1.2 g/30 mL) and 10 μL internal standard for injection into instrument.

For analytical measurement by LC-MS/MS, a Zorbax Eclipse C18 delay column (4.6 × 50 mm × 5 μm) was fitted between the LC pump and the autosampler and an injection volume of 100 μL was utilized. Chromatographic separation was achieved by an Eclipse C18 analytical column (4.6 × 75 mm × 3.5 μm). Mobile phase A consisted of 3% volume methanol in DI water and mobile phase B was methanol. The initial flow rate was 0.6 mL/min and mobile phase B was kept at 1% for 2 min and then increased to 60%, 85% and 99% at 3, 8.5 and 9 min, respectively, followed by a hold at 99% mobile phase B until 12.7 min. See Data S3 for additional information on analytical quantification and quality control.

Using the measured internal concentrations, bioconcentration factor (L/kg) was calculated as:

$$BCF = \frac{C_{embryo}}{C_{solution}}$$

where C_{embryo} is the chemical body burden (g/kg tissue), calculated from the measured internal concentration of pooled embryo samples divided by the number of embryos, 40, and multiplied by the mean wet weight of 48 hpf embryos, 0.27 ± 0.01 mg (Menger et al., 2019). Mean embryo wet weight was measured by pooling 80 or 100 embryos in a tube, removing all excess water, weighing by difference, and averaging for 4 replicates. $C_{solution}$ is the aqueous exposure concentration (g/L), as calculated from analytically verified stock solutions.